Hassan Vand and Tippner
Journal of Wood Science (2024) 70:39
https://doi.org/10.1186/s10086-024-02152-2

Journal of Wood Science

ORIGINAL ARTICLE

Open Access

Effects of moisture content on the behaviour of Scots pine heartwood and sapwood under impact

Mojtaba Hassan Vand[1*] and Jan Tippner[1]

Abstract

The material properties of sapwood and heartwood vary within various wood species and even they can show significant differences within a single tree. Scots pine (*Pinus sylvestris* L.), a species that plays a crucial role in timber production for joinery and building construction applications, is among those that show a notable distinction between its heartwood and sapwood. To examine the influence of moisture content (MC) on the impact behaviour of the sapwood and heartwood of pine, we tested specimens with two distinct moisture levels: a low moisture content (LMC) group with 12% MC and a high moisture content (HMC) group with 45% MC. In our study, we investigated deflection, normal strain and force development of the specimens during the short period of an impact, and also calculated the impact bending strength (IBS) of samples, using an impact testing machine equipped with a high-speed camera and digital image correlation method. Our results indicate that the differences between sapwood and heartwood at LMC were insignificant in the case of maximum deflection and normal strain, thus there is no need for differentiation; however, these differences became more pronounced, and non-negligible, with an increase in MC. We also evaluated the IBS of both heartwood and sapwood and found that, at LMC, heartwood had greater impact bending strength than sapwood, making it a preferable choice as a material subjected to impact loadings. Conversely, at HMC, both heartwood and sapwood would be equally strong against impacts, indicating that pine green wood shows no sensitivity to the ratio of sapwood to heartwood in the tree.

Keywords Scots pine, Heartwood, Sapwood, Impact, Strain rate, Moisture content, Digital image correlation, Duration of load, Impact bending strength

Introduction

Wood serves diverse functions in many industries—including aviation, automotive, construction, sports equipment and tool production—due to its capacity to withstand both static and dynamic loads [1]. Its inherent characteristics, such as resistance to splitting, stress concentration and crushability, make it a preferred material for applications like packaging [2]. Wood's ability to absorb impact and its eco-friendly aspects make it ideal for guardrail production [3]. Among the diverse wood species native to Eurasia, Scots pine (*Pinus sylvestris* L.) stands out for having the broadest geographic range in the region and significant global importance in timber production [4]. Scots pine wood is easy to handle and process; and it has adequate strength and is lightweight, making it an excellent choice for joinery and construction materials. Its sapwood can be effectively treated with preservatives, making it suitable for deteriorating environments, for example as railway sleepers and fencing [5]. The significance of Scots pine has led to comprehensive studies into various aspects of its properties, including its physical, mechanical and energy-related attributes [6].

*Correspondence:
Mojtaba Hassan Vand
xhassanv@mendelu.cz
[1] Faculty of Forestry and Wood Technology, Mendel University, Zemědělská 3, 613 00 Brno, Czech Republic

Toughness is the amount of energy a material can absorb and the impact test is the standard method for determining it, but it has no universal agreement about the details of its measurement and different national standardisation bodies have chosen different definitions [7]. The ability to absorb the energy of impact bending is called the impact bending strength (IBS), and shows how much the material has toughness against impact loadings [8]. IBS indicates the resistance of wood to crack propagation and it depends significantly on the hemicellulose level of the wood, which varies by species [9]. Moreover, IBS can be affected by the length of the span of a beam following a parabolic function [10]. Standardised impact testing can be a viable alternative to scaling between different methods; it can be used to focus on material behaviour and compare energy absorption [11]. The impact strength of the material, in the form of mechanical work applied for the rupture of the specimen, can be independently calculated by measuring the loss of kinetic energy of the drop weight due to impact loading [12]. The loading rate can affect the mechanical behaviour of wood, and studies present conflicting results on the effect of loading rate on wood strength [3, 13, 14].

As the tree ages and its trunk thickens, the more centrally located xylem undergoes a transformation process and becomes heartwood, while the outer zone of the xylem, which is younger, remains unchanged and is referred to as sapwood [15]. Events associated with heartwood formation include the death of parenchyma, the accumulation of gas, desiccation, cessation water transport, embolism, pit closure, ethylene production, enzyme activity, the depletion of storage compound, the removal or accumulation of elemental nutrients, the formation of extractives and the formation of tyloses [16]. In general, heartwood and sapwood are assumed to have the same mechanical properties despite some levels of difference in their material properties [17]. Heartwood, typically more affluent in extractives, tends to be drier, heavier and harder, and has a lower fibre saturation point and hygroscopicity than sapwood [18]. The mineral composition also varies, with higher levels of sodium and phosphorus in heartwood, while calcium and magnesium are more concentrated in sapwood [19]. In general, while the modulus of elasticity of sapwood is slightly higher than heartwood and heartwood exhibits greater hardness than sapwood, there is no significant difference in their modulus of rupture [20]. The pine heartwood is notably more resistance to water and decay exposure than sapwood (three times more resistant) [21]. The sapwood and heartwood of pine cannot be modified with the same method due to their differences in impregnation ability [22]. These significant differences in material properties lead to pine sapwood and heartwood being used for different applications [4]. The outer regions of the trunk have higher impact loading strength than the inner regions, and the lower parts of the trunk are stronger against impact loadings than the higher points of the trunk [23]. Given the crucial importance of Scots pine and the substantial differences between its sapwood and heartwood, a thorough examination of the two wood types was considered to be beneficial.

Historically, the primary approach to studying and analysing dynamic loadings was to determine equivalent static loading values. The static methods were adapted with slight modifications for application to dynamic loadings until specialised methods for impact loading were designed and developed [24]. Impact testing methods consist of three main types: drop weight testing machines (e.g., Fremont, Hatt-Turner and Olsen); pendulum impact testing machines (e.g., Amsler, Charpy and Izod); and flywheel testing as exemplified by the Guillery method [25]. Studies suggest that high strain-rate effects in timber become apparent only when strain rates exceed a certain level. In other words, up to a certain strain rate level, the material's mechanical behaviour may remain unaffected [26]. Wood is damage-tolerant as its fibre-bundle structure, with a weak interface between the fibres, prevents cracks from passing from one fibre to the next, thus isolating the crack [27]. While studies indicate that the strength of wood against impact loadings depends significantly on the species, the influence of growth-ring direction on strength varies across different studies [28, 29]. Among different species, scots pine's impact strength was also studied extensively due to its global importance [30]. The effect of temperature on IBS of different species can be an increase, decrease or no significant effect [1, 31].

Digital image correlation (DIC) is a technique that uses digital images acquired from the surface of an object to compare and analyse its movement and deformation [32]. The common strain gauges and extensometers which need to be installed on the specimens often have a considerable error and their output can be with a considerable inaccuracy [33]. Unlike strain gauges and extensometers, which need to be in contact with the specimen, DIC can provide strain distribution measurements without being affected by the motion of the specimen and testing machine [34]. DIC has substantial potential for evaluating finite element method modelling of wood by comparing its results with strain distribution and deflection results from experimental methods [35]. Originally, DIC was not intended for assessing impact loading dynamics. High-speed cameras were primarily utilized to gauge the velocity of the impactor pre- and post-impact, thereby assessing momentum transfer and kinetic energy loss [36]. However, by improvement of high-speed cameras to capture images, DIC emerges as a valuable tool for comprehensively evaluating impact loadings depicting strain distribution and specimen deflection [37]. This shift provides insights into the alterations within specimens during impact, surpassing previous methods that solely focused on the speed of the impacting object [38].

Methods

Production and preparation of samples

Wooden planks of Scots pine were obtained from a local sawmill affiliated with the Training Forest Enterprise Masaryk Forest Křtiny (Mendel University in Brno, Czech Republic). Special orthotropic blocks with dimensions of 300×20×20 mm (longitudinal×radial×tangential direction) were crafted from these boards. Samples of both heartwood and sapwood were taken from many different planks were included to ensure that the impact of each individual tree on the results was minimised. We inspected the specimens thoroughly, discarding those with knots or defects. Pine sapwood (PSW) and pine heartwood (PHW) samples were allocated to a low moisture content group (LMC) and a high moisture content group (HMC). The specimens in the LMC group were stored in an environment of 20 °C and 65% relative humidity until stabilising at equilibrium moisture content (EMC) of 12%. The specimens in the HMC group were submerged in water and then stored above the water in a closed compartment to achieve a moisture content of 40–60%. After the tests, the specimens underwent oven drying, and their EMC was calculated by measuring their weight before and after the drying process. Figure 1 displays one of the boards used for making the samples, clearly illustrating the heartwood and sapwood of the tree.

To demonstrate the microscopic differences between PSW and PHW, comparative photos can be highly informative. Figure 2 presents transverse sections of both PSW and PHW at two different magnification levels [39].

Impact test equipment

The tests were conducted using the DPFest 400 drop-weight impact testing machine (Labortech s.r.o., Czech Republic) at the Josef Ressel Research Centre in Brno Útěchov, Czech Republic. The test parameters were in accordance with Czech standards [40, 41]. The 9.05 kg hammer was released from a height of 815.7 mm, striking the samples with a velocity of 4 m/s, delivering 72.4 J of energy to them. A force sensor (CFTplus, manufactured by Hottinger Brüel and Kjaer, Austria) mounted on the hammer measured the reaction force at a sampling frequency of 1 MHz. Figure 3 shows the testing settings and the testing machine used for the impact test.

Fig. 1 Transverse section of one of the boards

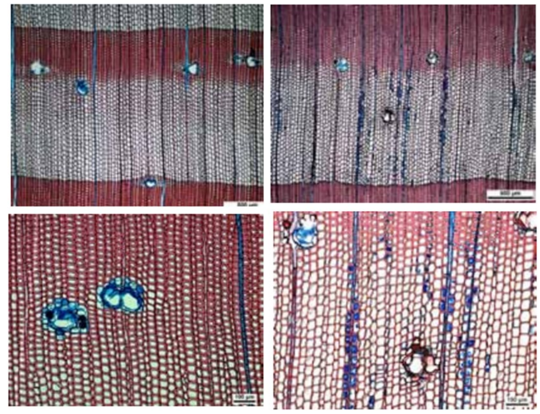

Fig. 2 Transverse section of sapwood (left) and heartwood (right) of scots pine

The room in which the samples were stored and tested was maintained at a standard room temperature of 20 °C. To examine the effect of growth-ring orientation on IBS, within each group, half of the samples were struck by the hammer parallel to their growth-ring orientation (impact force in the tangential direction), while for the other half it was perpendicular (impact force in the radial direction). Some research articles suggest that the orientation of the growth rings affects only the maximum force and not other parameters [42]. It is customary to divide the measured absorbed energy by the cross-sectional area of the sample to eliminate the influence of specimen dimensions in various tests, as shown in the following equation [43]:

$$\text{IBS}\ (\text{kJ/m}^2) = \frac{\textit{energy required to break the test sample}\ (\text{kJ})}{\textit{species cross section}(\text{m}^2)} \tag{1}$$

High-speed image capturing equipment

To capture a sufficient number of images within the brief duration of impact, we used a high-speed camera, specifically the Photron Fastcam SA-X2 1000k-M2 (Photron Ltd, Japan), equipped with a Nikon Micro-Nikkor G lens with a focal length of 105 mm (Nikon Corporation, Japan). This operates at a frame rate of 50,000 per second and offers a resolution of 768×328 pixels. Two high-speed MultiLED QT light sources were used to ensure a uniform light level, as minimising variations in lighting across the images was essential. We used the DIC method to measure the deflection and strain distribution of the samples. The DIC software Vic-2D version 2010

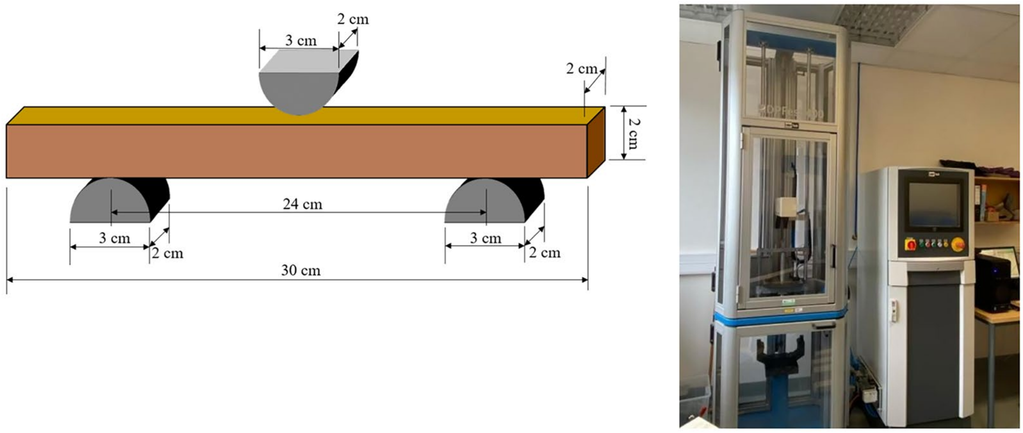

Fig. 3 Impact testing sample settings and the testing machine DPFest 400

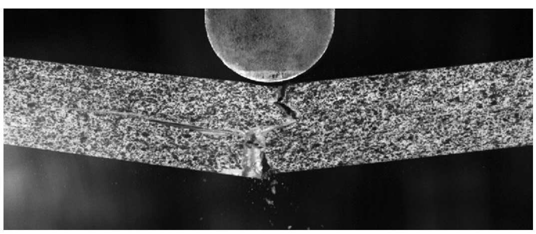

Fig. 4 Photograph of the impact of the hammer on one specimen

Table 1 Number and basic mechanical properties of samples in each group

	Number	Moist density (ρ_{12}) (kg/m^3)	Dried density (G_{12}) (kg/m^3)	MC (%)
PSW LMC	22	486.0 (42.1)	434.5 (36.0)	12.0 (1.1)
PHW LMC	21	575.9 (50.8)	506.3 (44.4)	13.2 (0.8)
PSW HMC	17	637.5 (48.3)	409.9 (29.4)	55.7 (13.9)
PHW HMC	14	665.2 (63.1)	473.0 (38.3)	40.6 (9.0)

(Correlated Solutions, Inc., USA) processed the images, using a simple scale calibration method to determine the conversion factor. Lagrange notation was used to compute the strain tensor of the specimens. Before testing, we painted the specimen surfaces with a randomly generated grey-scale speckled pattern. This pattern's quality directly impacts the image's output quality and consequently affects the accuracy of the DIC method [44]. The camera was positioned to ensure parallel alignment with the object surface, and any out-of-plane motion of the specimen during loading was minimised to a negligible level [45]. Figure 4 presents an image captured during crack propagation upon impact.

Results and discussion

Both PSW and PHW samples from the LMC and HMC groups underwent the same procedure to reach the required MC. However, the MC of PSW and PHW in both groups were different for the LMC and HMC groups. Table 1 shows the quantity of each group and their median of moisture content and density for each group, with their standard deviations presented in parentheses.

By comparing our tests with previous studies, it is evident that the densities of the samples in our study fall within a commonly encountered range. The median density shows a difference of 0.5%, 0.1% and 9% from the results of [10, 43, and 15], respectively. The individual values for the density of both groups show a 10.2% difference for sapwood and a 27% difference for heartwood from other research [18]. Table 1 shows that the density of the heartwood was 18.5% higher than sapwood, and after moisture absorption it was 4% denser than sapwood, also the sapwood absorbed more moisture than the heartwood.

Collecting and processing data from the testing machine and DIC software enabled us to obtain the required test results. The normal strain gave a distinct pattern in all beams, with the highest compressive value at the top and the highest tensional value at the bottom midpoint [46]. While the maximum tensional normal strain value was considerably less than the maximum absolute value of the compressive normal strain [47], cracks consistently began at the bottom of the samples due to the brittle nature of wood in tension [42]. Figures 5, 6, 7, 8 present the tensional normal strain and the deflection of beams over time, along with their maximum values up to the moment before crack initiation. All box-plots in this article indicate no outlier points. The box-plot charts depict the median as the central vertical line and the average of each group as a cross mark. Unfortunately, as far as the authors know, no published

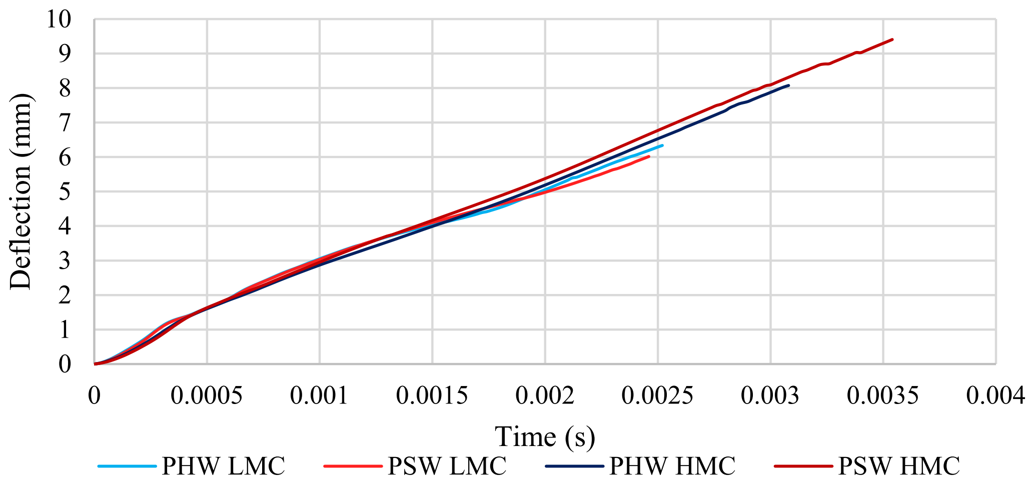

Fig. 5 Median of deflection vs. time by group

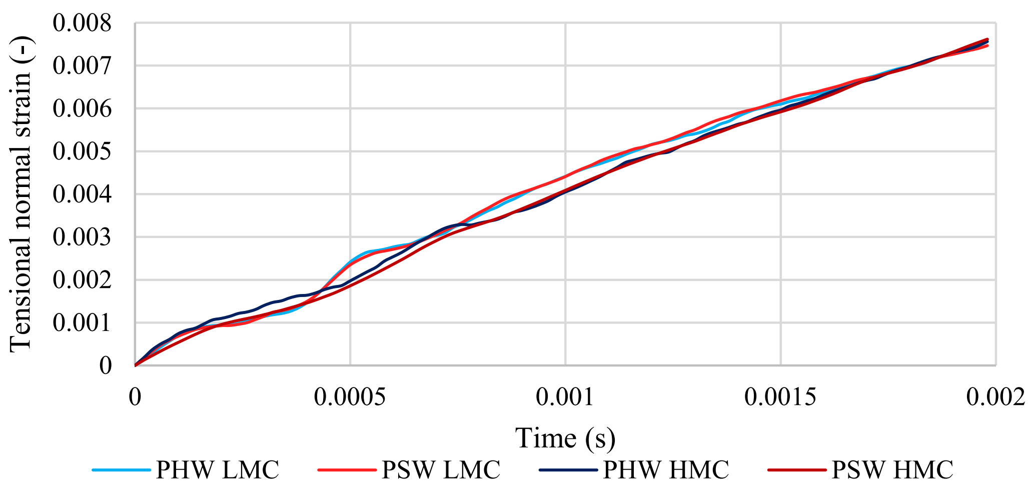

Fig. 6 Median of tensional normal strain vs. time by group

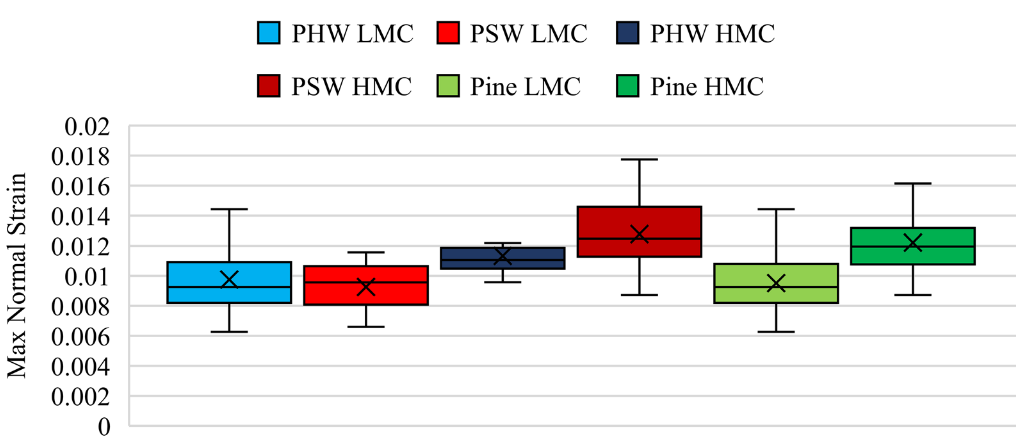

Fig. 7 Maximum tensional normal strain up to the breakage point

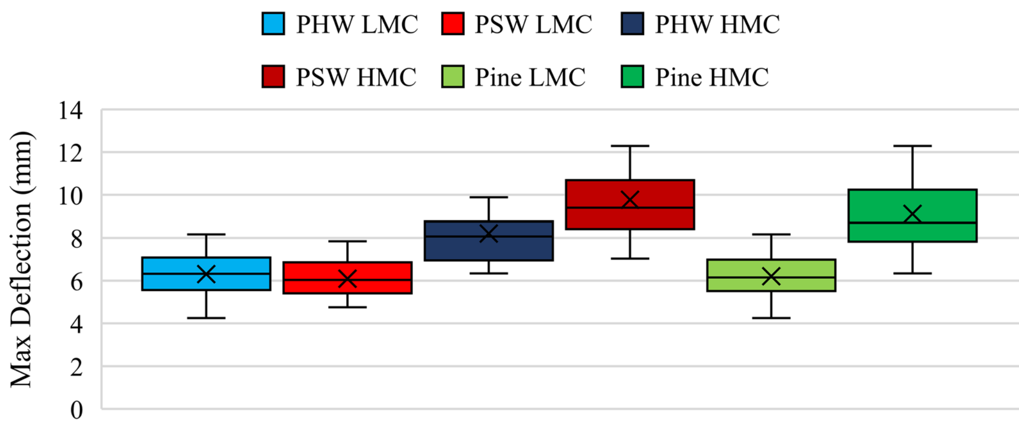

Fig. 8 Maximum deflection up to the breakage point

study describes the use of a high-speed camera and DIC for three-point bending impact loading of Scots pine with the same test settings, so our deflection and normal strain results cannot be compared with earlier studies.

Figures 5 and 6 show that, regardless of the maximum values of each group, the plots of all groups are almost identical. Essentially, the deflection and normal strain of the beams gave the same pattern for all groups and the main difference is the duration of the plots. Figures 7 and 8 highlight these differences and graphically display the comparative variances of maximum deflection and maximum normal strain. The maximum deflection and tensional normal strain values for both PSW LMC and PHW LMC show less than a 5% difference. However, for the HMC group, the disparity is more significant, exceeding 12%. By using the analysis of variance (ANOVA) test on the PSW and PHW sample results, the p-values were determined to be 0.05027 for PSW LMC and PHW LMC, and 0.0209 for HMC; which implies there is no significant difference between PSW LMC and PHW LMC, whereas for higher moisture content, there were statistically significant differences.

We measured the force inflicted on the beam using a force sensor located in the hammer of the testing machine. The onset of the impact always began with a peak followed by a trough, resulting from a slight hit followed by the detachment of the specimen. This small peak is called the "inertial peak" [48]. The brittle failure of the beam can suddenly release internal energy (i.e., it is elastic), causing a "negative deceleration", and these negative decelerations can manifest as negative forces in some charts [49]. Figures 9 and 10 depict the force vs. time charts for both LMC and HMC groups. The differences between PSW and PHW are negligible for the HMC samples, while for the LMC samples, the force vs. time charts show some differences. Figure 11 illustrates the box-plot

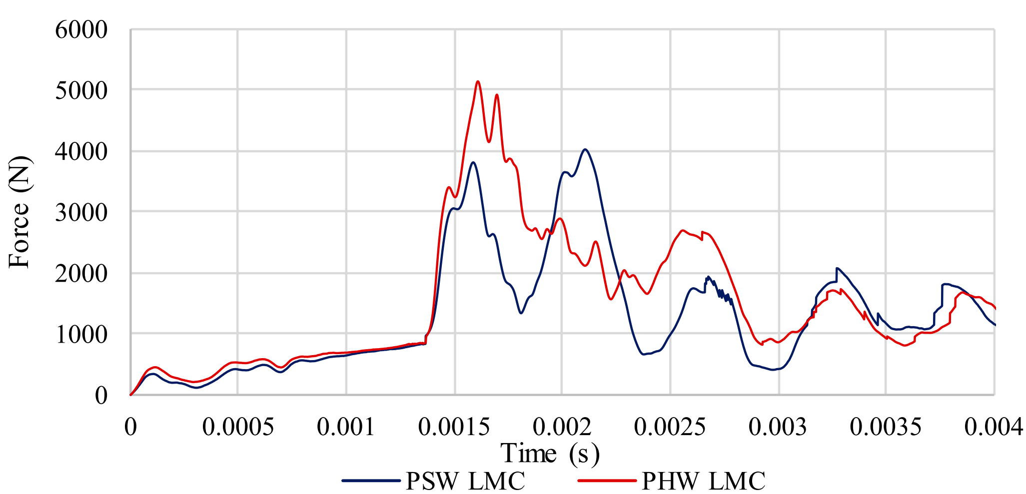

Fig. 9 Median of reaction force vs. time by LMC group

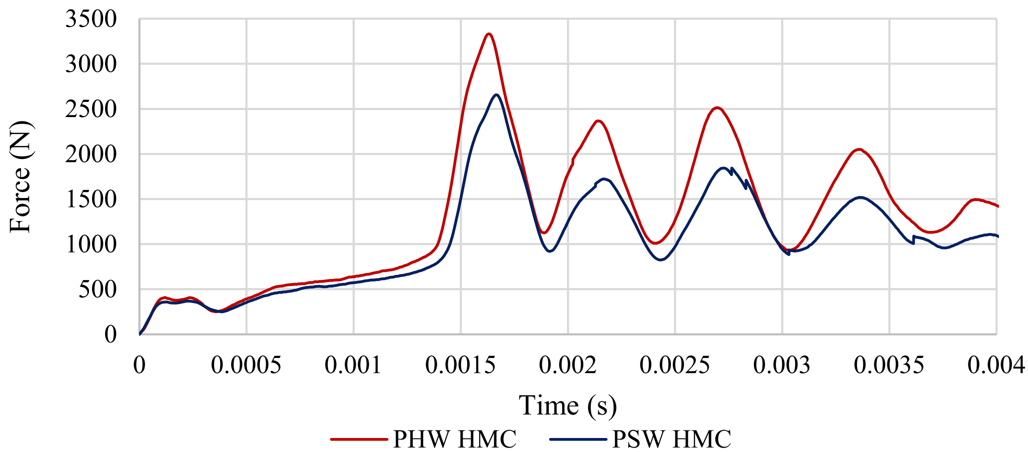

Fig. 10 Median of reaction force vs. time by HMC group

of the maximum reaction force of all groups. It can be observed that the maximum force for the LMC group has much more diverse values, while the HMC groups are more concentrated than the LMC, and the maximum force for them is less diverse. In Figs. 9, 10, and 11, the force plots for the LMC group show more significant differences than those for the HMC group. In other words, the plots for PHW and PSW become more similar with an increase in EMC. Also, the significant disparity in the size of the box-plots suggests that the LMC groups have a wider range, indicating a broader distribution and more scattered data compared to the HMC groups which this behavior is found in former studies [50]. It should be mentioned that the final median plot of the LMC force is more varied than HMC making the median chart more challenging to use than the HMC plot.

We determined the IBS of the samples by using the testing machine. Figure 12 shows the results of the samples by group indicating that, for both LMC and HMC groups, the IBS of heartwood is greater than sapwood. The IBS of both PSW and PHW increases with an increase in MC. An ANOVA test for IBS revealed that the p-value of IBS for PSW LMC and PHW LMC was 0.021, while for the HMC group it was 0.068. These values suggest that there was a difference between PHW LMC and PSW LMC, and there was no difference between PHW HMC and PSW HMC.

Figures 13 and 14 show the relationships between the density and IBS for two levels of MC (LMC and HMC). Based on the regression model, it can be stated that dependency of the IBS on density decreases with increasing the MC.

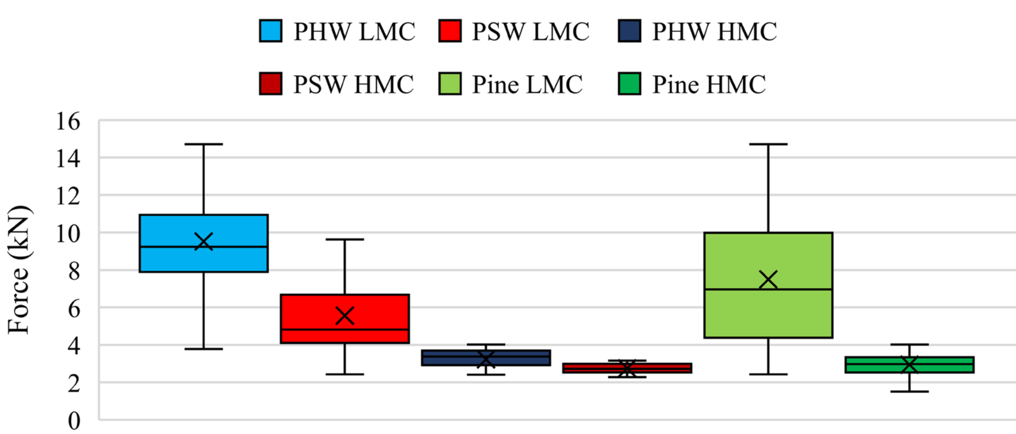

Fig. 11 Reaction force of samples up to the breakage point by group

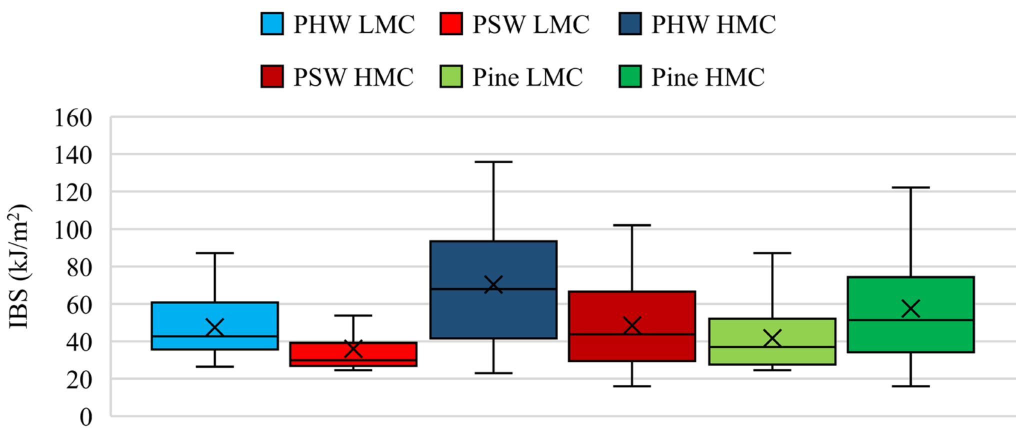

Fig. 12 IBS of samples by group

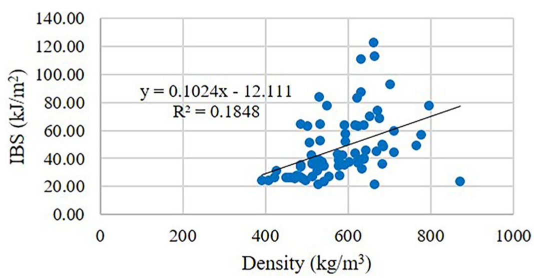

Fig. 13 IBS vs. time by LMC group

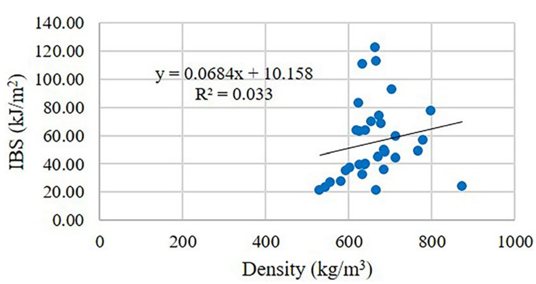

Fig. 14 IBS vs. time by HMC group

The power regression of the LMC group can be more efficient, providing a higher coefficient of determination, as shown in the following equation:

$$\begin{aligned} y &= 0.0016x^{1.4681} \\ R^2 &= 0.2896 \end{aligned} \quad (2)$$

Unlike deflection, strain and maximum force, the IBS of Scots pine has been determined by various researchers, providing a basis for comparison with our results. IBS values at 11% MC were reported as 35.7, 56.3, 72, 27.5, and 18.8 kJ/m^2 by authors [1, 10, 43, 51, 52], respectively, with our results showing differences of 3.5%, 52%, 94%, 25.6% and 49%, respectively. Another article offering a comprehensive perspective on the general material properties of sapwood vs. heartwood determined IBS for sapwood as 0.047 Nm/mm^2 and for heartwood as 0.029 Nm/mm^2 [18].

While our results are presented here in charts, reference to the values can also be helpful in interpreting the results. Table 2 presents the median values of the test results alongside their standard deviation.

Table 2 Median value and standard deviation of the results of the tests

	PHW LMC	PSW LMC	PHW HMC	PSW HMC	Pine LMC	Pine HMC
Max deflection (mm)	6.3 (1.1)	6.0 (1.1)	8.1 (1.5)	9.3 (2.2)	6.1 (1.1)	8.7 (2.1)
Max normal strain	0.00925 (0.0041)	0.00904 (0.0018)	0.0108 (0.0014)	0.01238 (0.0025)	0.00922 (0.0032)	0.01195 (0.0022)
Max force (kN)	9.2 (2.8)	4.8 (2.2)	3.4 (0.7)	2.7 (0.3)	7.0 (3.2)	3.0 (0.5)
IBS (kJ/m^2)	42.7 (16.6)	29.9 (14.1)	68.0 (34.6)	43.7 (23.0)	37.0 (16.4)	51.4 (30.3)

The results indicate that the maximum values of deflection, normal strain and IBS increase with an increase in moisture content. However, the maximum force required for breakage decreases. This moisture content effect aligns with the findings of former studies [50].

Conclusions

For Scots pine wood with a 12% MC, the ANOVA test showed that there is no significant difference between the maximum deflection and normal strain of PHW and PSW, and they exhibit similar behaviour. Thus, the maximum deflection and normal strain for pine LMC can be assumed to be 6.14 mm and 0.00925 without considering the percentage of the PSW and PHW. However, with higher MC, PSW demonstrates significantly more deflection and normal strain than PHW. It is noteworthy to mention that the maximum deflection and normal strain increase for both PSW and PHW with an increase in EMC.

The force vs. time charts of PHW LMC and PSW LMC show a substantial difference in the maximum force required for crack initiation. Nevertheless, as MC rises, the force–time charts of heartwood and sapwood become more similar, showing the same pattern as the maximum force required for crack initiation converges.

The IBS of PHW LMC (42.66 kJ/m^2) is approximately 30% more than that of PSW LMC (29.86 kJ/m^2), making heartwood a better choice for building materials under impact loadings. As the moisture content rises, IBS for both sapwood and heartwood lose their intensity, and the ANOVA test shows that there would be no difference between the PSW HMC and PHW HMC, confirming the assumption of 51.38 kJ/m^2 IBS for both PHW and PSW as correct.

Abbreviations

MC	Moisture content
IBS	Impact bending strength
LMC	Low moisture content
HMC	High moisture content
DIC	Digital image correlation
EMC	Equilibrium moisture content
PHW	Pine heartwood
PSW	Pine sapwood
ANOVA	Analysis of variance

Author contributions

All authors have accepted responsibility for the entire content of this manuscript and approved its submission.

Funding

This work was supported by the Ministry of Education, Youth and Sports of the Czech Republic [Grant Number #LL1909, ERC CZ].

Availability of data and materials

The data used in this study are available from the corresponding author on reasonable request.

Declarations

Ethics approval and consent to participate

Not applicable.

Competing interests

The authors declare no competing interests.

Received: 20 May 2024 Accepted: 31 July 2024
Published online: 15 August 2024

References

1. Özkan OE (2022) Effect of freezing temperature on impact bending strength and Shore-D hardness of some wood species. BioResources 17(4):6123
2. Johnson W (1986) Historical and present-day references concerning impact on wood. Int J Impact Eng 4(3):161–174
3. Leijten AJM (2004) Heat treated wood and the influence on the impact bending strength. Heron 49(4):349–360
4. Bieker D, Rust S (2010) Non-destructive estimation of sapwood and heartwood width in Scots pine (*Pinus sylvestris* L.). Silva Fenn 44(2):267–273
5. Savill PS (2019) The silviculture of trees used in British forestry. CABI, Wallingford
6. Warguła Ł, Wojtkowiak D, Kukla M, Talaśka K (2020) Symmetric nature of stress distribution in the elastic-plastic range of *Pinus* L. pine wood samples determined experimentally and using the finite element method (FEM). Symmetry 13(1):39
7. Polocoşer T, Kasal B, Stöckel F, Li X (2018) Dynamic material properties of wood subjected to low-velocity impact. Mater Struct 51:1–16
8. Gaff M, Kačík F, Gašparík M (2019) Impact of thermal modification on the chemical changes and impact bending strength of European oak and Norway spruce wood. Compos Struct 216:80–88
9. Hughes M, Hill C, Pfriem A (2015) The toughness of hygrothermally modified wood. Holzforschung 69(7):851–862
10. Bal BC (2021) Effect of span length on the impact bending strength of poplar and pine woods. BioResources 16(2):4021
11. Polocoşer T, Stöckel F, Kasal B (2016) Low-velocity transverse impact of small, clear spruce and pine specimens with additional energy absorbing treatments. J Mater Civ Eng 28(8):04016048
12. Widmann R, Steiger R (2009) Impact loaded structural timber elements made from Swiss grown Norway spruce. In: Proceedings of CIB-W18 Meeting, vol 42.
13. Green DW, Winandy JE, Kretschmann DE (1999) Mechanical properties of wood. In: Wood Handbook – Wood as an Engineering Material (Gen. Tech. Rep. FPL-GTR-113). U.S. Department of Agriculture Forest Products Laboratory, Madison, WI.
14. Büyüksarı Ü (2017) Effect of loading rate on mechanical properties of micro-size Scots pine wood. BioResources 12(2):2721–2730
15. Niemz P, Teischinger A, Sandberg D (eds) (2023) Springer handbook of wood science and technology. Springer, Heidelberg
16. Taylor AM, Gartner BL, Morrell JJ (2002) Heartwood formation and natural durability – a review. Wood Fiber Sci 34(4):587–611
17. Kretschmann D (2010) Mechanical properties of wood. Wood handbook: wood as an engineering material: chapter 5. Centennial ed. General technical report FPL; GTR-190. Madison, WI: US Dept. of Agriculture, Forest Service, Forest Products Laboratory, 2010: p. 5.1–5.46., 190, pp.5–1
18. Bektaş İ, Tutuş A, Gültekin G (2020) The effect of sapwood and heartwood differences on mechanical properties of fast-growing tree species. Wood Ind/Drvna Ind 71(3):249–259
19. Meerts P (2002) Mineral nutrient concentrations in sapwood and heartwood: a literature review. Ann For Sci 59(7):713–722
20. Esteves B, Nunes L, Domingos I, Pereira H (2014) Comparison between heat treated sapwood and heartwood from *Pinus pinaster*. Maderas Cienc Tecnol 16(3):311–322
21. Sehlstedt-Persson M, Wamming T (2010) Wood drying process: impact on Scots pine lumber durability. J Wood Sci 56:25–32

22. Matsumura J, Booker RE, Ridoutt BG, Donaldson LA, Mikajiri N, Matsunaga H, Oda K (1999) Impregnation of radiata pine wood by vacuum treatment II: effect of pre-steaming on wood structure and resin content. J Wood Sci 45:456–462
23. De Palacios P, Esteban LG, Guindeo A, Navarro N (2008) Variation of impact bending in the wood of *Pinus sylvestris* L. in relation to its position in the tree. For Prod J 58(3):37–44
24. Kalthoff JF (1985) On the measurement of dynamic fracture toughnesses – a review of recent work. Int J Fract 27:277–298
25. Siewert TA, Manahan MP, McCowan CN, Holt JM, Marsh FJ, Ruth EA (2000) The history and importance of impact testing. ASTM Spec Tech Publ 1380:3–16
26. Jacques E, Lloyd A, Braimah A, Saatcioglu M, Doudak G, Abdelalim O (2014) Influence of high strain-rates on the dynamic flexural material properties of spruce–pine–fir wood studs. Can J Civ Eng 41(1):56–64
27. Bruck HA, Evans JJ, Peterson ML (2002) The role of mechanics in biological and biologically inspired materials. Exp Mech 42:361–371
28. Borůvka V, Novák D, Šedivka P (2020) Comparison and analysis of radial and tangential bending of softwood and hardwood at static and dynamic loading. Forests 11(8):896
29. Hassan Vand M, Tippner J, Brabec M (2024) Effects of species and moisture content on the behaviour of solid wood under impact. Eur J Wood Wood Prod 82(1):23–34
30. Bragov AM, Gonov ME, Igumnov LA, Konstantinov AY, Lomunov AK, Yuzhina TN (2023) Experimental and computational study of deformation and fracture of pine under dynamic three-point bending of beams. Deformation and destruction of materials and structures under quasi-static and impulse loading. Springer, Cham, pp 83–99
31. Baumann G, Brandner R, Müller U, Stadlmann A, Feist F (2021) A comparative study on the temperature effect of solid birch wood and solid beech wood under impact loading. Mater 14(24):7616
32. Zhang D, Arola DD (2004) Applications of digital image correlation to biological tissues. J Biomed Opt 9(4):691–699
33. Kubojima Y, Kato H, Tonosaki M (2002) Proportional limit of wood obtained from a load-time diagram during an impact bending test. J Wood Sci 48:527–531
34. Dave MJ, Pandya TS, Stoddard D, Street J (2018) Dynamic characterisation of biocomposites under high strain rate compression loading with split Hopkinson pressure bar and digital image correlation technique. Int Wood Prod J 9(3):115–121
35. Timbolmas C, Rescalvo FJ, Portela M, Bravo R (2022) Analysis of poplar timber finger joints by means of Digital Image Correlation (DIC) and finite element simulation subjected to tension loading. Eur J Wood Wood Prod 80(3):555–567
36. Olmedo I, Bourrier F, Bertrand D, Toe D, Berger F, Limam A (2015) Experimental analysis of the response of fresh wood stems subjected to localised impact loading. Wood Sci Technol 49:623–646
37. Mindess S, Madsen B (1986) The fracture of wood under impact loading. Mater Struct 19:49–53
38. Wouts J, Haugou G, Oudjene M, Morvan H, Coutellier D (2018) Strain rate effects on the compressive response of wood and energy absorption capabilities – Part B: experimental investigation under rigid lateral confinement. Compos Struct 204:95–104
39. Merela M, Turičnik V, Vek V, Oven P (2019) Anatomske, kemijske in sorpcijske lastnosti beljave in jedrovine rdečega bora. Acta Silvae et Ligni 119:43–54
40. ČSN 490115 (1979) Wood. Detection of static bending strength. Czech Standards Institute, Prague (**in Czech**)
41. ČSN 490117 (1980) Wood. Impact strength in bending. Czech Standards Institute, Prague (**in Czech**)
42. Hassan Vand M, Tippner J (2023) Impact bending strength of thermally-modified timber. Holzforschung 77(11–12):828–837
43. Bollmus S, Beeretz C, Militz H (2020) Tensile and impact bending properties of chemically modified Scots pine. Forests 11(1):84
44. Sutton MA, Orteu JJ, Schreier H (2009) Image correlation for shape, motion and deformation measurements: basic concepts, theory and applications. Springer, Berlin
45. Pan B, Qian K, Xie H, Asundi A (2009) Two-dimensional digital image correlation for in-plane displacement and strain measurement: a review. Meas Sci Technol 20(6):062001
46. Schneeweiß G, Felber S (2013) Review on the bending strength of wood and influencing factors. Am J Mater Sci 3:41–45
47. Iraola B, Cabrero JM (2016) An algorithm to model wood accounting for different tension and compression elastic and failure behaviours. Eng Struct 117:332–343
48. Marsavina L, Sadowski T, Kneć M, Negru R (2010) Non-linear behaviour of foams under static and impact three point bending. Int J Non Linear Mech 45(10):969–975
49. Baumann G, Brandner R, Müller U, Kumpenza C, Stadlmann A, Feist F (2020) Temperature-related properties of solid birch wood under quasi-static and dynamic bending. Mater 13(23):5518
50. Hassan Vand M, Tippner J (2024) The effect of moisture content over the fibre saturation points on the impact strength of wood. R Soc Open Sci 11(2):231685
51. Korkut S, Akgül M, Dündar T (2008) The effects of heat treatment on some technological properties of Scots pine (*Pinus sylvestris* L.) wood. Bioresour Technol 99(6):1861–1868
52. Kamperidou V, Barboutis I, Vasileiou V (2014) Influence of thermal treatment on mechanical strength of Scots pine (*Pinus sylvestris* L.) wood. Wood Res 59(2):373–378

Publisher's Note